

Natural Products

# Isolation and Total Synthesis of Icumazoles and Noricumazoles—Antifungal Antibiotics and Cation-Channel Blockers from *Sorangium cellulosum*\*\*

Jenny Barbier, Rolf Jansen, Herbert Irschik, Stefan Benson, Klaus Gerth, Bettina Böhlendorf, Gerhard Höfle, Hans Reichenbach, Jens Wegner, Carsten Zeilinger, Andreas Kirschning,\* and Rolf Müller\*

Myxobacteria are a potent source of secondary metabolites<sup>[1]</sup> of which the genus *Sorangium* has yielded the largest number.<sup>[2]</sup> In the course of our ongoing bioactivity-guided screening program, an unknown antifungal spectrum of activity was detected in the extract of *S. cellulosum*, So ce701, and led to the isolation of the unique isochromanone- and oxazole-containing icumazoles (**1a–c**).<sup>[3]</sup> Later the same characteristic structural element was rediscovered in the noricumazoles (**2a,b**).

Here, we provide a concise report on the icumazoles (**1a–c**) and noricumazoles (**2a–c**) which covers their isolation and structure elucidation as well as studies on their ion-channel-inhibitory properties. We approached these goals utilizing a broad range of strategies based on various spectroscopic methods and the chemical determination of relative and absolute configurations by derivatization, degradation, and fragment synthesis, and unequivocally by the total synthesis of noricumazole A (**2a**). In addition, we provide evidence for the ion-channel-inhibitory effect of noricumazole A (**2a**) utilizing a new screening concept for oligomeric ion channels.

For the production of icumazoles (**1a–c**) the producer was cultivated at 30 °C for 14 days in a 100 L fermentor, and icumazoles were isolated as described in the Supporting Information. Icumazoles (**1a–c**) are easily recognized in

UPLC-DAD-UV analyses (ultra-performance liquid chromatography with diode array UV detection) by their UV spectra, especially by the intense main absorption at 302 nm with side bands at 290 and 316 nm, which are characteristic for conjugated short polyenes. In the high-resolution ESIMS, the signal for the molecular ion  $M^+$  of the peak eluting at  $R_t = 15.37$  min indicated the molecular formula  $C_{33}H_{45}NO_7$  for icumazole A (**1a**), which was fully compatible with the NMR data (Table S1 in the Supporting Information). The 33 carbon signals in the <sup>13</sup>C NMR spectrum were classified according to the DEPT spectrum, and three heteroatom-bound exchangeable protons were calculated, which were not visible in the <sup>1</sup>H NMR spectra in [D<sub>4</sub>]MeOH. All protons in the <sup>1</sup>H NMR spectra could be unambiguously assigned to their corresponding carbon atoms from their correlations in the <sup>1</sup>H,<sup>13</sup>C HMQC spectrum. The correlations in the <sup>1</sup>H,<sup>1</sup>H COSY spectrum provided four major domains (A–D; Figure 1). The remaining unsaturated methine singlet (H19,  $\delta_{H/C} = 7.80/138.0$  ppm) was recognized as part of a heteroaromatic ring because of its large <sup>1</sup>J<sub>HC</sub> coupling constant of 209 Hz. Along with the quaternary carbon atoms C18 and C20 next to one nitrogen and one oxygen atom, this methine C19 forms an oxazole

[\*] Dr. R. Jansen,<sup>[4]</sup> Dr. H. Irschik, Dr. K. Gerth, B. Böhlendorf,<sup>[5]</sup> Prof. Dr. G. Höfle, Prof. Dr. H. Reichenbach, Prof. Dr. R. Müller  
Helmholtz-Zentrum für Infektionsforschung (HZI)  
Arbeitsgruppe Mikrobielle Wirkstoffe  
Inhoffenstrasse 7, 38124 Braunschweig (Germany)  
E-mail: rom@mx.uni-saarland.de

J. Barbier,<sup>[4]</sup> Dr. S. Benson, J. Wegner, Prof. Dr. A. Kirschning  
Institut für Organische Chemie und Zentrum für Biomolekulare  
Wirkstoffe (BMWZ)  
Leibniz-Universität Hannover  
Schneiderberg 1B, 30167 Hannover (Germany)  
E-mail: andreas.kirschning@oci.uni-hannover.de

Dr. C. Zeilinger  
Institut für Biophysik, Leibniz-Universität Hannover  
Herrenhäuser Strasse 2, 30419 Hannover (Germany)

[†] Current address: DSM Nutritional Products Ltd.  
R&D Human Nutrition and Health, Basel (Switzerland)

[‡] These authors contributed equally to this work.

[\*\*] This work was funded by the Fonds der Chemischen Industrie (scholarship for J.W.).

Supporting information for this article is available on the WWW under <http://dx.doi.org/10.1002/anie.201106435>.

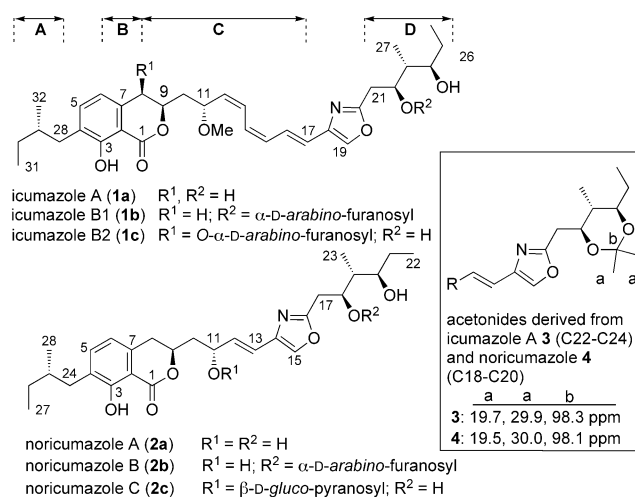


**Figure 1.** Icumazoles A–B2 (**1a–c**), noricumazoles A–C (**2a–c**), and acetonides **3** and **4** with relevant <sup>13</sup>C NMR data and determination of relative stereochemistry (stereochemistry shown as elucidated in this paper; numbering does not relate to IUPAC numbering; for clarity reasons the depicted numbering was chosen; A–D refer to NMR domains).

ring, which links units C and D as indicated by their  $^1\text{H}$ ,  $^{13}\text{C}$  HMBC correlations (Table S1 with figure). HMBC correlations between oxymethine C11 and the methoxy group C33 established the ether group at position C11 in unit C. Based on the HMBC correlations of structural elements A, B, and C and of the remaining quaternary carbon atoms, the isochromanone system was established. Although direct evidence for a ring closure between C1 and C9 could not be drawn from the HMBC spectrum, only a lactone ring can account for the low-field shift of H9 ( $\delta = 4.83$ ) and for the chemical shift of C1 ( $\delta = 172.1$ ). The *Z,Z,E* configuration of the triene unit in **1a** was derived from the vicinal coupling constants  $J_{12,13}$  and  $J_{14,15} = 11\text{--}12$  Hz and  $J_{16,17} = 15.2$  Hz. A ROESY correlation between H17 and H19 showed the cisoidal stereochemical relation of the oxazole methine C19 and the triene methine C17.

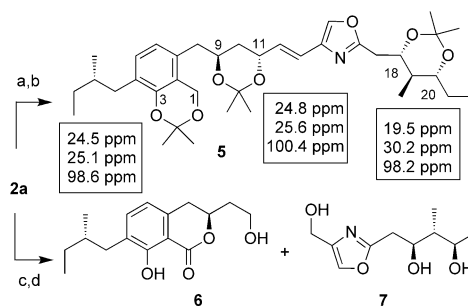
Additionally, two more-polar icumazoles were recognized during analyses of extracts along with considerable amounts of carolacton.<sup>[4]</sup> The elemental composition  $\text{C}_{38}\text{H}_{53}\text{NO}_{11}$  of icumazole B1 (**1b**) ( $R_t = 14.0$  min) accounts for an additional  $\text{C}_5\text{H}_8\text{O}_4$  unit, which suggested the presence of a pentosyl residue. Based on a comparison of  $^1\text{H}$  and  $^{13}\text{C}$  NMR data of **1b** (Table S2 in the Supporting Information) with the literature values, we propose an  $\alpha$ -arabino-furanosyl residue.<sup>[5]</sup> Details on the structure elucidation of **1b** and **1c** are discussed in the Supporting Information.

In contrast to icumazoles (**1a–c**), the characteristic oxazole-triene chromophore (290, 302, 316 nm) was missing in the UV spectrum of noricumazole A (**2a**). The elemental composition  $\text{C}_{28}\text{H}_{39}\text{NO}_7$  was determined by high-resolution ESIMS from the  $[\text{M}+\text{H}]^+$  ion cluster at  $m/z$  502.2797 (calcd. 502.2799). The NMR data of the isochromanone and oxazole units in **2a** were identical to those measured for icumazole A (**1a**) (Table S4 in the Supporting Information). However, the lower mass of metabolite **2a** (by 66 Da, which corresponds to  $\text{C}_5\text{H}_6$ ) relative to the mass of **1a** is associated with the replacement of the methoxyl by a hydroxy group and the loss of both *Z* double bonds. According to the ROESY correlation H13/H15, the cisoidal conformation between H13 at the last *E* double bond and the oxazole 15H remains similar to that in **1a–c**. In analogy to the icumazoles, two more-polar derivatives were isolated in addition to noricumazole A (**2a**) ( $R_t = 12.6$  min). Noricumazole B (**2b**) ( $R_t = 11.4$  min) was identified as the 18*O*- $\alpha$ -arabino-furanoside related to icumazole **1b** (Table S5) and noricumazole C (**2c**) ( $R_t = 10.9$  min) is a 11*O*- $\beta$ -gluco-pyranoside (for details see the Supporting Information and Table S6).<sup>[6]</sup>

Neither icumazole A (**1a**) nor noricumazole A (**2a**) provided suitable crystals for X-ray crystallographic analysis. Therefore, we had to elucidate the stereochemistry of all stereogenic centers by a chemical approach that focused on noricumazole A (**2a**), which is chemically more stable than triene **1a**.

We used acetonides **3** (**1a**, 2,2-dimethoxypropane, *p*TsOH, RT, 60 min, 73%) and **4** (**2a**, 2,2-dimethoxypropane, *p*TsOH, RT, 15 min, 67%) to determine the relative configuration of the 1,3-diol moiety by Rychnovsky's method (Figure 1).<sup>[7]</sup> The relative stereochemistries at C22–C24 in **3** and C18–C20 in **4** were both determined to be *anti,anti* as

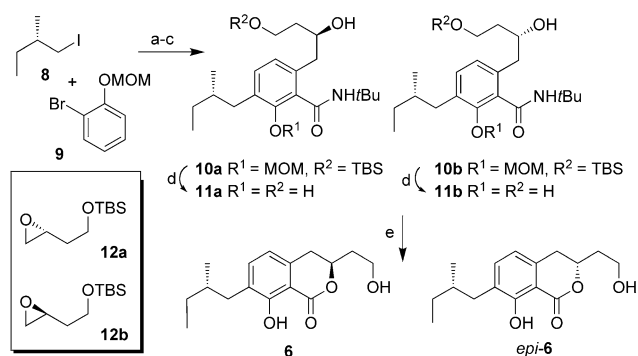
judged from the  $^{13}\text{C}$  NMR data and the relevant  $^1\text{H}$ ,  $^1\text{H}$  coupling constants ( $J_{22,23} = 10.3$  Hz and  $J_{23,24} = 10.1$  Hz for **3**;  $J_{18,19} = 10.4$  Hz and  $J_{19,20} = 10.0$  Hz for **4**<sup>[8]</sup>). Next, noricumazole A (**2**) was transformed into trisacetonide **5** and fragments **6** and **7** by a set of standard transformations (Scheme 1). Derivative **5** confirmed the relative configuration at C18–C20



**Scheme 1.** Preparation of acetonide **5** and relevant  $^{13}\text{C}$  NMR data and preparation of fragments **6** and **7** from noricumazole A (**2a**). Reagents and conditions: a) **2a**,  $\text{LiBH}_4$ , THF,  $0^\circ\text{C}$ , 10 min; b) 2,2-dimethoxypropane, *p*TsOH, RT, 10 h, 18% (for two steps); c) **2a**, NMO,  $\text{K}_2\text{OsO}_4 \cdot 2\text{H}_2\text{O}$ , *t*BuOH,  $\text{H}_2\text{O}$ ,  $0^\circ\text{C}$  to RT, 4 h, 45%; d) 1.  $\text{NaIO}_4$ , THF, 1.5 h; 2.  $\text{NaBH}_4$ ,  $\text{CH}_2\text{Cl}_2/\text{MeOH}$  (3:1), RT, 1 h, 32% of **6**, 98% of **7**. NMO = 4-methylmorpholine *N*-oxide, Ts = tosyl.

of noricumazole A (**2a**) and established the *anti* orientation of the diol at C9 and C11. Then, the fragments **6**, its diastereomer *epi*-**6**, and **7** were independently synthesized and compared with the authentic samples collected from the oxidative fragmentation. The syntheses established the absolute configuration of all stereogenic centers including the isolated one at C25.

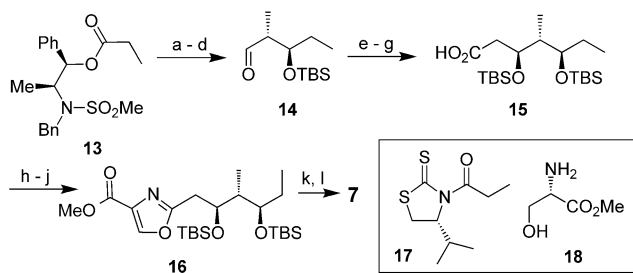
The phenolic precursor **9** was first modified by three successive organometallic transformations introducing the three C substituents (Scheme 2). The  $\text{sp}^3\text{--sp}^2$  cross-coupling reaction with (*S*)-iodide **8**<sup>[9]</sup> required lithiation of the bromide and worked best with MOM protection of the phenol group. After substantial optimization, the iron-catalyzed version<sup>[10,11]</sup> of the Kumada reaction<sup>[12]</sup> gave the cross-coupling product in excellent yield. The second *ortho* position was functionalized again by lithiation followed by treatment with *tert*-butyl isocyanate. The resulting amide then served to direct another *ortho* lithiation and alkylation employing both enantiomeric oxiranes **12a,b**<sup>[13,14]</sup> which independently yielded adducts **10a** and **10b**, respectively.  $\delta$ -Lactones **6** and *epi*-**6** were formed after removal of all *O*-protecting groups, and the resulting phenols **11a** and **11b** were cyclized under acidic conditions. Importantly, the C24 protons differed for epimers **6** and *epi*-**6** in the  $^1\text{H}$  NMR spectrum and thus were used as a diagnostic criterion for elucidating the relative stereochemistry between C25 and C9.<sup>[15]</sup> Comparison (NMR and CD spectroscopy; see Figure S1) with fragment **6** obtained from the oxidative fragmentation of noricumazole A (**2a**) revealed the identity of natural and synthetically derived **6** and established the absolute configuration of the stereogenic centers at C25 and C9 to be *S*. Consequently, the configuration at C11 was assigned to be *R* with reference to acetonide **5**. If one assumes stereochemical identity of icumazole A (**1a**) and noricumazole A (**2a**), the configuration at C11 is also *R*.



**Scheme 2.** Preparation of western fragments **6** and *epi-6*. Reagents and conditions: a) 1. (*S*)-**8**, Mg, THF, Δ, 1 h; 2. **9**, HMTA, TMEDA, [Fe(acac)<sub>3</sub>], 0 °C, 1.5 h, 98%; b) 1. *n*BuLi, TMEDA, Et<sub>2</sub>O, −30 °C, 2 h, then 3 h at −5 °C; 2. *t*BuNCO (10 equiv), RT, 14 h, 94%; c) *n*BuLi (3 equiv), TMEDA (3 equiv), Et<sub>2</sub>O, −78 °C to −40 °C, 2 h, then addition of (*S*)-**12** (2 equiv), −78 °C to −40 °C, 14 h, **10a** 73% (99% based on recovered starting material), likewise using **12b** yields **10b** 81%; d) HCl<sub>conc</sub>, EtOH, 50 °C, 2.5 h, **11a** 89%, **11b** 94%; e) *p*TsOH, toluene, Δ, 30 min, **6** 89%, *epi-6* 95%. acac = acetylacetonate, HMTA = hexamethylphosphorus triamide, MOM = methoxymethyl, TMEDA = tetramethylethylenediamine.

zole A (**2a**) one can conclude that the additional stereogenic center at C8 in **1c** is *R*.

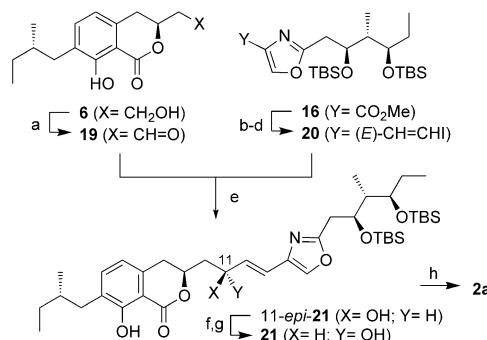
The synthesis of the stereotriade in fragment **7** relied on the Masamune *anti* aldol reaction<sup>[16]</sup> and the Nagao acetate aldol reaction<sup>[17]</sup> (Scheme 3) starting from propionate **13** and propanal. The Nagao aldol reaction with aldehyde **14** using thioxothiazolidine **17** furnished carboxylic acid **15** after *O*-silylation and hydrolytic removal of the chiral auxiliary. This was coupled with serine methyl ester **18** and transformed to methyl ester **16** in good overall yield by DAST-mediated



**Scheme 3.** Synthesis of the eastern fragment **7**. Reagents and conditions: a) *c*-HexBOTf, NEt<sub>3</sub>, propanal, CH<sub>2</sub>Cl<sub>2</sub>, −78 °C, 2 h, 91%, d.r. > 20:1; b) TBSOTf, 2,6-lutidine, CH<sub>2</sub>Cl<sub>2</sub>, −78 °C to RT, 50 min, quant.; c) DIBAL-H, CH<sub>2</sub>Cl<sub>2</sub>, −78 °C, 30 min, 91%; d) Dess–Martin periodinane, CH<sub>2</sub>Cl<sub>2</sub>, RT, 1 h; e) **17**, TiCl<sub>4</sub>, *i*Pr<sub>2</sub>EtN, −40 °C to −78 °C, 1.5 h; f) TBSOTf, 2,6-lutidine, CH<sub>2</sub>Cl<sub>2</sub>, −78 °C, 30 min, 91% over three steps; g) 1 M LiOH, 30% H<sub>2</sub>O<sub>2</sub>, THF/H<sub>2</sub>O 4:1, 0 °C to RT, 12 h, 99%; h) **18**, HOBT, TBTU, *i*Pr<sub>2</sub>EtN, CH<sub>2</sub>Cl<sub>2</sub>, RT, 12 h, 97%; i) DAST, CH<sub>2</sub>Cl<sub>2</sub>, −78 °C, 3 h, 78% (88% based on recovered starting material); j) DBU, BrCCl<sub>3</sub>, CH<sub>2</sub>Cl<sub>2</sub>, 0 °C to RT, 6 h, 85%; k) DIBAL-H (2 equiv), CH<sub>2</sub>Cl<sub>2</sub>, −78 °C, 1 h, quant.; l) BF<sub>3</sub>·OEt<sub>2</sub>, CH<sub>3</sub>CN, 0 °C, 7 h, 72%. DAST = diethylaminosulfur trifluoride, DBU = 1,8-diazabicyclo[5.4.0]undec-7-ene, Hex = *n*-hexyl, HOBT = hydroxybenzotriazole, TBSOTf = *t*-butyldimethylsilyl triflate, TBTU = *O*-benzotriazol-yl-*N,N,N',N'*-tetramethyluronium tetrafluoroborate.

cyclization and aromatization. Finally, the ester **16** was transformed into the desired triol **7**, and its relative configuration and identity was proven by comparison of the NMR data with that of the degradation fragment **7** (Figure S2a in the Supporting Information). The absolute configurations (1*S*,19*R*,20*R*) were further substantiated by identical optical rotations (natural fragment: [α]<sub>D</sub><sup>20</sup> = −22.5, *c* = 0.2, MeOH); synthetic fragment: [α]<sub>D</sub><sup>20</sup> = −20.8, *c* = 0.2, MeOH) and CD spectroscopy (see Figure S2 in the Supporting Information).

Finally, the structure of noricumazole A (**2a**) was unequivocally confirmed by total synthesis (Scheme 4). This was achieved by fusing vinyl iodide **20** with aldehyde **19**



**Scheme 4.** Completion of the total synthesis of noricumazole A (**2a**). Reagents and conditions: a) Dess–Martin periodinane, NaHCO<sub>3</sub>, CH<sub>2</sub>Cl<sub>2</sub>, 0 °C, 45 min, 85%; b) DIBAL-H, CH<sub>2</sub>Cl<sub>2</sub>, −78 °C, 1 h, quant.; c) K<sub>2</sub>CO<sub>3</sub>, Ohira–Bestmann reagent, MeOH, 0 °C to RT, 86%; d) Schwartz reagent, THF, 0 °C, 1 h, then NIS, −78 °C, 25 min, 94%; e) *t*BuLi, **20**, Et<sub>2</sub>O, −78 °C, 1 h, then Me<sub>2</sub>Zn, −78 °C, 15 min, then **19**, Et<sub>2</sub>O, −78 °C, 2.5 h, 74%, d.r. = 1:1 (**21**/*11-epi-21*); f) *11-epi-21*, PPh<sub>3</sub>, *p*-nitrobenzoic acid, DEAD, THF, 0 °C to RT, 3 h, 90%; g) NaOH, H<sub>2</sub>O, THF/MeOH (2:1), 0 °C, 12 h, 92%; h) **21**, BF<sub>3</sub>·Et<sub>2</sub>O, CH<sub>3</sub>CN, 0 °C, 12 h, 90%. DEAD = diethyl azodicarboxylate, NIS = *N*-iodosuccinimide, TBS = *tert*-butyldimethylsilyl.

(obtained from the western fragment **6** under strictly acid- and water-free conditions) via the corresponding vinyl zinc intermediate, which was generated by transmetalation of the lithiated vinyl iodide using Me<sub>2</sub>Zn. It yielded the desired product **21** and its epimer *11-epi-21* (d.r. = 1:1).<sup>[18]</sup> Methyl ester **16** was elaborated to the vinyl iodide **20** by reduction to the corresponding aldehyde followed by Seyferth–Gilbert homologation<sup>[19]</sup> using Bestmann's reagent.<sup>[20]</sup> The resulting alkyne was subjected to a *syn*-hydrozirconation<sup>[21]</sup> followed by iodination. After chromatographic separation of the two diastereomers, the undesired isomer *11-epi-21* was directly converted into **21** by Mitsunobu inversion<sup>[22]</sup> which was combined with ester hydrolysis. This sequence improved the yield of the desired coupling product **21** to 68%. Completion of the synthesis was achieved by Lewis acid mediated TBS removal<sup>[23]</sup> to furnish noricumazole A (**2a**) in 15% overall yield over 15 steps (longest linear sequence) (including Mitsunobu inversion: 17 steps and 26% overall yield).

The physical and analytical data of the product obtained by total synthesis were identical with those recorded for authentic noricumazole A (**2a**),<sup>[24]</sup> thus establishing the absolute configurations of all stereogenic centers of noricumazole

(**2a**) as depicted in Figure 1. Based on chemical and biosynthetic considerations it can be expected that these assignments match the stereochemistry of the icumazoles (**1a–c**).

Assessment of the biological properties of icumazole A (**1a**) revealed activity (minimum inhibitory concentration (MIC) in  $\mu\text{g mL}^{-1}$ ) against various fungi, for example, *Mucor hiemalis* (1.25), *Botrytis cinerea* (0.04), *Pythium debaryanum* (0.3), *Sclerotinia sclerotiorum* (1.25) (selected from Table S7 in the Supporting Information), and the yeast-like *Rhodotorula glutinis* (0.3). Experiments with *R. glutinis*, which grows as single cells, showed that **1a** inhibited growth but did not act fungicidal even at tenfold concentration of the MIC (Figure S3 in the Supporting Information).<sup>[25]</sup> However, DNA, RNA, and protein syntheses were blocked immediately after addition of icumazole A (**1a**), probably because of inhibition of a basic metabolic process. Consequently, the influence of **1a** on the oxidation of NADH in cell-free preparations of mitochondria from *R. glutinis* was studied; it was found that NADH oxidation was inhibited with a maximal inhibition of 60–70% at a concentration of about  $5 \text{ ng mL}^{-1}$  (Figure S4 in the Supporting Information). Similar behavior had been observed with myxothiazol acting on membranes of *Paracoccus denitrificans*.<sup>[25b]</sup> In principle, complete inhibition did not occur because several redundant fungal pathways for the oxidation of NADH can exist.<sup>[26]</sup>

In contrast, noricumazole A (**2a**) does not exert marked antibiotic activity. Surprisingly, we found that noricumazole A (**2a**) is able to stabilize the tetrameric form of the potassium channel (KcsA) in a temperature-dependent manner. About half of all tetrameric KcsA ion channels dissociate into their monomers at  $82^\circ\text{C}$ .<sup>[27]</sup> In contrast, in the presence of noricumazole A (**2a**) KcsA tetramers and even oligomers are formed at lower temperatures ( $50\text{--}80^\circ\text{C}$ ) and remain stable up to  $90^\circ\text{C}$  as judged by SDS-PAGE (see Figure S5 in the Supporting Information). To the best of our knowledge, this is the first example in which a natural product induces such a stabilization of the KcsA architecture. It is only known that sodium chloride has a similar effect, and in contrast potassium chloride stabilizes the KcsA channel.<sup>[28,29]</sup>

To connect this unusual activity of noricumazole A (**2a**) to a biological function, a fluorescence assay was established that relies on a potassium sensing fluorescence dye (PBFI) used to detect potassium transport in reconstituted biological systems.<sup>[30]</sup> Liposomes were charged with PBFI and the purified ion channel KcsA was integrated into the artificial membrane, thus forming channelsomes. In the presence of potassium chloride (1M added to the assay to yield 0.5M final concentration) potassium ions are transported inside the channelsomes and the fluorescence signal was monitored (see Figure S6A in the Supporting Information). In the absence of KcsA, control liposomes showed only a weak response to the presence of potassium ions (see Figure S6A). Addition of noricumazole A (**2a**) to the channelsomes led to a reduction of the fluorescence signal and this effect was dose dependent (see Figure S6A).<sup>[31]</sup> The concentration-dependent inhibitory effect ( $\text{IC}_{50}$ ) of noricumazole A (**2a**) on the ion channel KcsA was determined to be  $4 \mu\text{M}$ , while the  $\text{IC}_{50}$  value for sodium

chloride is 85 mM and for nickel chloride 190 mM (see Figure S6C).

These results indicate that noricumazole A (**2a**) stabilizes the architecture of KcsA and inhibits the transport of potassium cations through the ion channel. The latter result was further confirmed in electrophysiological measurements because noricumazole A (**2a**) completely inhibits single-channel activity at  $1 \mu\text{M}$  concentration (Figure S7 in the Supporting Information).<sup>[32]</sup> These values are in the same range as those reported for other specific ion-channel inhibitors like the scorpion toxin charybdotoxin, which exerts a 10- to 100-fold higher affinity to human potassium channels.<sup>[33]</sup>

In conclusion, icumazole A (**1a**) and noricumazole A (**2a**) along with two glycosylated congeners are new oxazole- and isochromanone-containing metabolites from different *S. cellululosum* strains. The aglycons in **1a** and **2a** differ only by the presence of a methoxy or a hydroxy group at C11 and in the length of the central triene or monoene units. The absolute configuration of noricumazole A (**2a**) was unequivocally elucidated by total synthesis of noricumazole A (**2a**).

Our initial experiments suggest that icumazole A (**1a**) targets the respiratory chain while noricumazole A (**2a**) exerts potassium-ion-channel inhibitory activity which may be related to its stabilizing property of the KcsA architecture.

Received: September 11, 2011

Published online: December 23, 2011

**Keywords:** antibiotics · ion-channel inhibitors · myxobacteria · natural products · structure elucidation · total synthesis

- [1] S. C. Wenzel, R. Müller, *Curr. Opin. Drug Discovery Dev.* **2009**, *12*, 220–230.
- [2] K. Gerth, S. Pradella, O. Perlowa, S. Beyer, R. Müller, *J. Biotechnol.* **2003**, *106*, 233–253.
- [3] H. Reichenbach, G. Höfle, B. Böhlendorf, H. Irschik, Ger. Pat 4 305 486A1, **1994**; CA **1994**, *121*, 3000667v.
- [4] R. Jansen, H. Irschik, V. Huch, D. Schummer, H. Steinmetz, M. Bock, T. Schmidt, A. Kirschning, R. Müller, *Eur. J. Org. Chem.* **2010**, 1284–1289.
- [5] a) S. Ek, H. Kartimo, S. Mattila, A. Tolonen, *J. Agric. Food Chem.* **2006**, *54*, 9834–9842; b) R. C. Beier, B. P. Mundy, *J. Carbohydr. Chem.* **1984**, *3*, 253–266.
- [6] G. J. Gerwig, J. P. Kamerling, J. F. G. Vliegthart, *Carbohydr. Res.* **1978**, *62*, 349–357.
- [7] R. D. Rychnovsky, B. N. Rogers, T. I. Richardson, *Acc. Chem. Res.* **1983**, *31*, 9–17.
- [8] The absolute configuration of the carbinol at C11 in **4** could not be determined by the Mosher ester method because epimerization occurred under the esterification conditions: H. Dale, S. Mosher, *J. Org. Chem.* **1973**, *38*, 2143–2147.
- [9] Iodide **7** was prepared from the corresponding alcohol: V. Martischonok, G. G. Melikyan, M. Alfred, O. Vostrowsky, H. J. Bestmann, *Synthesis* **1991**, 560–564.
- [10] G. Cahiez, V. Habiak, C. Duplais, A. Moyeux, *Angew. Chem.* **2007**, *119*, 4442–4444; *Angew. Chem. Int. Ed.* **2007**, *46*, 4364–4366.
- [11] W. M. Czaplak, M. Mayer, M. A. von Wangelin, *Angew. Chem.* **2009**, *121*, 616–620; *Angew. Chem. Int. Ed.* **2009**, *48*, 607–610.
- [12] Review: A. Fürstner, *Angew. Chem.* **2009**, *121*, 1390–1393; *Angew. Chem. Int. Ed.* **2009**, *48*, 1364–1367.

- [13] J. A. Frick, J. B. Klassen, A. Bathe, J. M. Abramson, H. Rapoport, *Synthesis* **1992**, 621–623.
- [14] K. Mori, M. Ikunaka, *Tetrahedron* **1984**, *40*, 3471–3479.
- [15] In addition, the two epimers showed different optical rotations: **6** [ $\alpha$ ]<sub>D</sub><sup>20</sup> = –33.0 (*c* = 0.1 g cm<sup>–3</sup>, CHCl<sub>3</sub>) and *epi-6* [ $\alpha$ ]<sub>D</sub><sup>20</sup> = +15.2 (*c* = 0.5, CHCl<sub>3</sub>).
- [16] T. Inoue, J.-F. Liu, D. C. Buske, A. Abiko, *J. Org. Chem.* **2002**, *67*, 5250–5256.
- [17] Other asymmetric variants with chiral ligands failed as a result of poor diastereocontrol (d.r. not better than 1:1.5) (also see the Supporting Information).
- [18] Y. Nagao, Y. Hagiwara, T. Kumagai, M. Ochiai, *J. Org. Chem.* **1986**, *51*, 2391–2393.
- [19] J. C. Gilbert, U. Weeresooriya, *J. Org. Chem.* **1979**, *44*, 4997–4998.
- [20] S. Müller, B. Liepold, G. J. Roth, H. J. Bestmann, *Synlett* **1996**, 521–522.
- [21] D. W. Hart, J. Schwartz, *J. Am. Chem. Soc.* **1974**, *96*, 8115–8116.
- [22] O. Mitsunobu, *Synthesis* **1981**, 1–28.
- [23] S. A. King, B. Pipik, A. S. Thompson, *Tetrahedron Lett.* **1995**, *36*, 4563–4566.
- [24] For details, including NMR spectra of mixtures of synthetic and natural **2a**, refer to the Supporting Information.
- [25] A similar effect had been observed with the antifungal myxothiazol: a) G. Thierbach, H. Reichenbach, *Antimicrob. Agents Chemother.* **1981**, *19*, 504–507; b) G. Thierbach, H. Reichenbach, *Arch. Microbiol.* **1983**, *134*, 104–107.
- [26] B. Maresca, A. M. Lambowitz, G. S. Kobayashi, G. Medoff, *J. Bacteriol.* **1979**, *138*, 647–649.
- [27] D. M. Cortes, E. Perozo, *Biochemistry* **1997**, *36*, 10343–10352.
- [28] F. I. Valiyaveetil, Y. Zhou, R. MacKinnon, *Biochemistry* **2002**, *41*, 10771–10777.
- [29] M. L. Renart, F. N. Barrera, M. L. Molina, J. A. Encinar, J. A. Poveda, A. M. Fernández, J. Gómez, J. M. González-Ros, *J. Biol. Chem.* **2006**, *281*, 29905–29915.
- [30] P. Jezek, F. Mahdi, K. D. Garlid, *J. Biol. Chem.* **1990**, *265*, 10522–10526.
- [31] The ion-channel-activity of icumazole A (**1a**) could not be tested because of its low chemical stability and partial degradation in the assays.
- [32] C. Zeilinger, M. Steffens, H.-A. Kolb, *Biochim. Biophys. Acta Biomembr.* **2005**, *1720*, 35–43.
- [33] Other established channel blockers like TBA, TEA, and Ba<sup>2+</sup> require higher concentrations than noricumazole A (**2a**) for inhibiting the KcsA channel.